



Contents lists available at BioMedSciDirect Publications

International Journal of Biological & Medical Research

Journal homepage: www.biomedscidirect.com



Original Article

Effect of MEV electron beam irradiation on fracture healing of tibia bone of rabbit

Suwendu Kumar Sahoo ^a, Biswajit Mallick ^b, Indramani Nath ^c, Rabi Narayan Mukharjee ^d

^aSenior Medical Radiation Physicist, Deptt. of Radiotherapy, HCG Panda Curie Cancer Hospital, Cuttack, Odisha, India

^bScientist, Institute of Physics, Sachivalaya Marg, Bhubaneswar, Odisha, India

^cProfessor, Department of Surgery and Radiology, College of Veterinary Science & Animal, Husbandry, OUAT, Bhubaneswar, Odisha, India

^dProfessor in Physics, School of Applied Sciences, KIIT University, Bhubaneswar, Odisha, India

ARTICLE INFO

Keywords:

MEV ELECTRON BEAM
FRACTURE HEALING
X-RAY DIFFRACTION
FOURIER TRANSFORM INFRARED
SPECTROSCOPY
DOSE

ABSTRACT

The study was undertaken by taking six numbers of clinically healthy eight to twelve months old New Zealand white rabbits of either sex, weighing about 1-2 kg body weight. The animals were provided with standard diet and maintained under uniform managerial conditions. A destruction of one tibia bone was done of all rabbits. Then (two male and one female) fracture sites of the three rabbits were irradiated with single fraction 0.5 Gy dose by 4 MeV Electron beam using Linear Accelerator after proper immobilization just after fracture of bone. Other three rabbits (two male and one female) were taken as control samples. X-Rays diffraction and Fourier Transform Infrared Spectroscopy analysis techniques were used for confirmation of particular 0.5 Gy dose for irradiation. The results of radiological image and clinical findings indicated that the fracture healing occurred faster in all rabbits with MeV electron irradiation than in those without irradiation. It is due to more accumulation of bone forming material like both inorganic hydroxyapatite and organic collagen at fracture site after electron beam irradiation.

© Copyright 2010 BioMedSciDirect Publications IJBMR -ISSN: 0976:6685. All rights reserved.

1. Introduction

Electron beam irradiation technologies have long been used for biomaterial applications [1] in different fields. The interaction of electron beam with matter shows various effects. The radiation induced effects in biomaterials include recombination of microorganisms, elimination of microorganisms associated with spoilage and contamination, sterilization of medically important proteins without affecting them and many more. Radiation processing refers to the use of radiation to change the properties of materials. When radiation passes through materials it breaks chemical bonds. Most precise and technically suitable electron beam can be obtained from the modern linear accelerator (Linac) meant for therapeutic use. Applications of electron beam irradiation include cross linking or recombination of microorganisms to improve or provide unique properties of biomaterial systems like other materials. Bone marrow is the soft flexible tissue biomaterial that lies within the hollow interior of long bones. This marrow is mainly responsible not only for new bone formation but also for fracture healing. The importance and high cost of treating bone fractures has promoted the development

of non-invasive methods of assessing fracture risk and prevention [2]. Bone marrow stem cells residing in the bone marrow are the progenitors for osteoblasts [3-5]. Autologous bone marrow injection to fracture site is a safe, simple and reliable method for treating delay and nonunion [6-8]. Again, the effect of bone marrow with low power laser irradiation also accelerates the fracture healing or bone binding process [5-6]. This is because of increase in recombination (of biomolecules) density among the cells in fracture site due to laser irradiation. This appeared by altered osteoblast activity at the fracture site as reflected by alkaline phosphate activity [9]. Laser irradiation also caused a significant increase in calcium accumulation at the fracture site [10].

So far as our knowledge is concerned; there is no report on electron beam irradiation with bone marrow to accelerate the fracture healing process of bone. The majority of the bone is made of the bone matrix. It is composed primarily of inorganic hydroxyapatite and organic elastic protein called collagen. The MeV electron beam is a high energy charge particle beam. When the fracture site is irradiated with this beam along with autologous bone marrow, the healing process becomes faster than the low energy laser therapy. This is because of more accumulation of both inorganic hydroxyapatite and organic collagen at fracture site.

* Corresponding Author :**Suwendu Kumar Sahoo**

D-66, METRO SATELLITE CITY, HANS PAL,
BHUBANESWAR, ODISHA, INDIA, PIN: 752101
suwendusahoo40@gmail.com,

MATERIALS AND METHODS:

In our study, in the first phase, we have extracted bone marrow from few rabbits and stored it in liquid nitrogen (-196°C) environment. The extracted bone marrow was then irradiated with 4 MeV electron beam from a modern linear accelerator by using a special instrumental attachment which has been designed and fabricated by us. This instrumental attachment facilitates irradiation of liquid samples at very low temperature (-196°C, liquid nitrogen) and has been presented schematically in figure 2. Then the modified bone marrow sample has been characterized by X-ray diffraction (XRD) and Fourier Transform Infrared Spectroscopy (FTIR) techniques for confirmation of dose. In the second phase of our study, the tibia bones of six rabbits were fractured under local anesthesia and usual surgical procedure and then irradiated with MeV electron beam. Subsequent clinical examination and weekly radiological studies were performed for the fracture site to determine the stage of fracture healing.

Bone marrow is a biomaterial which is a very soft and flexible tissue that lies within the hollow interior of long bones. This marrow is mainly responsible not only for new bone formation but also for fracture healing of the bone. In this work, we have used rabbit bone marrow as a sample of the experiment.

Collection of bone marrow sample:

In the first phase of experiment, the study was undertaken by taking eight numbers of clinically healthy eight to twelve months old New Zealand white rabbits of either sex, weighing about 1-2 kg body weight. The animals were provided with standard diet and maintained under uniform managemental conditions. The surgical procedure was performed under general anesthesia. All the animals were anaesthetized using mixture of ketamine hydrochloride @ 35 mg/kg body weight and xylazine hydrochloride @ 5 mg/kg body weight intramuscularly. Anesthesia was maintained by additional dose of intravenous ketamine hydrochloride whenever required. Medial aspect of proximal femur was shaved, cleaned and prepared aseptically for the surgical procedure. A two to three cm long skin incision was made on the medial aspect of the femur bone. The muscles were separated and the femur bone was exposed. Then bone marrow was extracted from both femoral bones of all rabbits by bone marrow needles. The sample was stored in liquid nitrogen till irradiation.

Bone fracture:

In the second phase of the experiment, six numbers of clinically healthy eight to twelve months old New Zealand white rabbits of either sex of 1-2 kg body weight were taken. Their diet and maintenance procedure were same as before. All the animals were anaesthetized using mixture of ketamine hydrochloride @ 35 mg/kg body weight and xylazine hydrochloride @ 5 mg/kg body weight intramuscularly. Anaesthesia was maintained by additional dose of intravenous ketamine hydrochloride whenever needed. The animals were restrained in lateral recumbency. Medial aspect of proximal tibia was shaved, cleaned and prepared aseptically for the

surgical procedure. A two to three cm long skin incision was made on the medial aspect of the limb below tibial tuberosity. The muscles were separated and the tibia bone was exposed. A length of 5 mm was marked in the anterior border of tibial diaphysis. Complete bone defect was created in that marked piece of the bone with the help of a heck saw without any bone fixation. Cold normal saline solution was poured at the site during osteotomy procedure to avoid thermal necrosis. Medio-lateral radiograph was also taken for confirmation of the bone defect and for comparison during healing process. Skin wound was closed in standard manner. All the animals were administered with antibiotic Sulphadiazine-Trimethoprim @ 50 mg/kg body weight intramuscularly once daily for 5 consecutive days and analgesic meloxicam @ 0.5mg/kg body weight intramuscularly once daily for at least 3 days. The skin incision wound was dressed daily with povidone-iodine solution until the complete healing of the incision site and sutures were removed on 10th day. After bone breaking two male rabbits and one female rabbit were irradiated with a dose of 0.5 Gy of MeV electron beam with proper immobilization in same day and other two male and one female rabbits were taken as control without irradiation. The dose 0.5 Gy is permissible dose for bone marrow. Regular clinical examination and weekly radiological image studies were performed for the fracture site to determine the stage of fracture healing.

MeV Electron beam irradiation at Liquid Nitrogen Environment

Experiment was carried out using 4 MeV electrons from a Modern Linac (Elekta, UK) installed at the Hemalata Hospitals and Research Centre (HHRC), Bhubaneswar, India. The Linac is capable to provide dual energy photon beams (6 MV and 15 MV) and electron beams of multiple energies (4, 6, 9 and 12 MeV) equipped with multi-leaf collimators (MLC) facility. The indigenously designed low temperature liquid irradiation cell (LTLIC) was used for irradiation purpose. The successful application of this attachment has been reported elsewhere [11]. The total irradiation work has been carried out in liquid nitrogen temperature environment. At very low temperature the radiation heating of the sample could be minimized, which reduced the cell death and biological defects in the liquid sample.

Engineering design of LTLIC

A specially designed cell for liquid sample irradiation is shown in Figure 1. The major parts of the special cell consist of a water tube, perspex (C₅H₈O₂) cell, volume adjusting syringe and liquid nitrogen (LN₂) container. The "water tube" is made of a plastic cylinder (special grade and non reactive to acid/base medium) with 0.5 mm thickness, 9 mm internal diameter, 10 mm external diameter and 15 mm length (graduated). One side of the water tube is closed with 3μ mylar film with the help of adhesive (Fevikwik). The liquid cell is made of a perspex sheet of 10 mm thickness and 50 50 mm² area.

A 10 mm free-hole was drilled at the centre of the perspex sheet to hold the volume adjusting syringe which is a commercially available special type of syringe (3ml volume with least measurement unit of 0.1ml) and is chemically inactive. The advantage is that because of adjustment provision, very less amount (μ) of liquid sample can be mounted for irradiation with the help of the micro syringe. Again a co-centric blind hole of 30 mm diameter and 8 mm depth was drilled to make a circular path for flow of LN_2 . A thin steel pipe of outer diameter 3 mm, internal diameter 2 mm and 50 mm length was taken to connect liquid cell with the LN_2 container. This makes a continuous flow of liquid nitrogen around the sample in a controlled manner. The LN_2 container of the LTLIC as shown in Fig. 2 is made up of thermocool material, which can hold LN_2 for 6-8 hours easily. The thermocool box is of internal volume 101014 cm^3 and outer volume 140140 cm^3 with a capacity of 1 liter LN_2 . Once filled, it can cool the materials in LTLIC for 1 hour during irradiation.

In first phase during irradiation of bone marrow, the LTLIC was put on the couch of Linac and the sample was put on sample space and below the mylar foil. High energy electron beam of energy 4 MeV has been used to irradiate the liquid biomaterial. The beam was collimated with field size of 22 cm^2 and allowed to fall on the liquid sample vertically. This attachment consists of a liquid cell made of mainly Styrofoam. The liquid sample studied here is bone marrow (50μ of rabbit) which was filled in a cylindrical perspex container with variable volume adjustment and fixed with Styrofoam in front of the beam line. The cylindrical water tube was placed on top of the sample for proper dose buildup. The total irradiation work was done at LN_2 environment (around -196 oC). The LN_2 was allowed to flow around the sample and the liquid sample became solid during irradiation. A pulse beam of 4 MeV electrons was used to irradiate the bone marrow at a dose rate of 300 MU/min for few seconds to build up a dose of 0.2 Gy, 0.5 Gy, 1.0 Gy, 2.0 Gy and 5.0 Gy per fraction to different samples for modification. The above vertical electron beam was allowed to fall on the liquid sample (bone marrow) after passing through the water tube (1cm) to provide maximum (100%) radiation dose to liquid sample, because the maximum dose build up length of 4 MeV electron beam is 1cm in water medium. This is because the penetrating length of 4 MeV electrons in bone marrow fluid is about 2.25 cm. But in second phase of our work, electron dose of 0.5 Gy was delivered to fracture site of tibia bone to all three rabbits after proper fixation in one fraction.

X-ray Diffraction and Fourier Transform Infrared Spectroscopy techniques were used for characterization of the modified samples. The spectroscopic data were analyzed by using origin 7.0 software. The X-Ray diffraction experimental setup consists of a grazing incidence X-ray instrument, i.e., GIXRD (next-generation Bruker AXS, D8 ADVANCE™ X-ray instrument) operated with monochromator in non-dispersive arrangement in parallel beam geometry with a resolution of 210^{-3} used for the inelastic scattering study. We used above diffractometer for our sample

study at Institute of Physics, Bhubaneswar. The grazing-angle geometry is characterized by the deep penetration of X-rays into materials; hence the yield of inelastically scattered quanta drastically increases. In this geometry, the sample was mounted in a two-axis goniometer; scanning was done by holding the angle of incidence constant (48.19°) and varying the diffraction angle 2θ ($= 96.34^\circ$) about the Bragg angle. Incident line focus $\text{CuK}\alpha$ radiation from a high-power X-ray tube operated at 1600 W (40 kV and 40 mA) using a KRYSTALLO 780 X-ray generator was used. Again, source with the Be-window of the high-power tube having 95% transmissions emits $\text{CuK}\alpha$ X-ray photons in the order of 1.2×10^{16} photon/s (considering only 1% of power converted to polychromatic $\text{CuK}\alpha$ X-rays). The CuK excitation from the line-focus tube, then the X-ray beam was collimated through fixed-divergence slit of 6 mm ($\approx 3^\circ$) before irradiating the sample. The scattered X-ray beam from the sample was well collimated by passing through Soller slit of 0.23° before getting it reflected by LiF (100) crystal monochromator ($d = 2.2265 \text{ \AA}$). A NaI dynamic scintillation counter of quantum yield around 95% was mounted on the arm of the goniometer circle of radius 300 mm. Step size chosen for this experiment was 0.05° with scan rate of $0.05^\circ/\text{min}$ (step). In this arrangement, X-rays are reflected from both the specimen and the focusing monochromator; which is known as reflection-reflection mode in double-crystal spectrometry (+1 -1). The observed spectral data were collected using a fully computer-controlled system and analyzed using software supplied by Bruker AXS, USA. The FTIR spectral measurement of all rabbit bone marrow samples were carried out at the sophisticated analytical instrumentation facility, Institute of Physics Bhubaneswar, by using AVTAR-CSI (Thermo Nicolet) Spectrometer in 4 cm^{-1} (Resolution) and auto gain mode. The spectra were recorded in the mid infrared region $4000\text{-}500 \text{ cm}^{-1}$ in transmittance mode. The sample (1 mg) was placed on KCL pellet which was made by six ton pressure. For digital X-Ray radiological image of the fractured bone of rabbit, we used Philips BV-300 C-Arm digital X-Ray Unit.

Results and Discussion:

X-Ray Diffraction Analysis

X-ray diffraction (XRD) technique was used to study the phase evolution and phase identification. The sample bone marrow of rabbit was studied for phase identification in GIXRD (next-generation Bruker AXS, D8 ADVANCE™ X-ray instrument) diffractometer operated with monochromator in non-dispersive arrangement in parallel beam geometry with a resolution of 2×10^{-3} used for the inelastic scattering study. The X-ray diffraction was used to investigate the organic collagen (Col) fibril distribution and orientation and also the presence of inorganic Hydroxyapatite (HA) in the bone marrow sample after MeV electron beam irradiation with different doses (0.0 cGy, 10 cGy, 50 cGy, 100 cGy, 200 cGy and 500 cGy).

The X-ray diffraction pattern of the virgin sample is given in figure 3 which shows the presence of collagen and HA (JCPDS 09-0432). The diffraction pattern at $2\theta = 5.62^\circ$ with d value 15.71 Å shows the presence of HA [23]. There were two nearer peaks at diffraction angles (2θ) of about 6.990 and 8.910 in this pattern. The first one and the second both are sharp peaks which are in accordance with the characteristic diffraction peaks of collagen. As per Bragg equation $2d \sin \theta = n\lambda$ ($\lambda = 1.54 \text{ \AA}$), the minimum values (d) of the repeat spacing were calculated. The d value of both peaks were 12.63 Å and 9.91 Å (table no.1) respectively which were related to the diameter of the tri-helix collagen molecule and the single left hand helix chain [24]. This collagen in the bone marrow sample is the tri-helix structure. The other two peaks at different diffraction angles 2θ (18.38° and 24.080) show the presence of HA with spacing value 4.82 Å and 3.69 Å. From this X-ray diffraction spectral analysis concepts it is very much clear that, the bone forming materials like inorganic material HA and organic material like collagen are present.

The X-rays diffraction pattern of the sample after 0.1 Gy MeV electron beam irradiation given in figure 4, which shows the presence of collagen and HA. But one collagen peak at $2\theta = 6.99^\circ$ is vanishing as compared to virgin sample.

The bone marrow sample after 0.5 Gy irradiation by electron beam, the XRD Pattern given in figure 5, the peak at diffraction angle 9.42° (Peak shown in figure 5 by arrow) shows the presence of pristine collagen [25] and which is a sharp peak. But this peak is not available in virgin and 0.1 Gy patterns. The peaks at diffraction angles 16.53° , 23.12° and 25.28° with corresponding spacing (d) value 5.35 \AA , 3.52 \AA and 3.43 \AA (Given in table no.3) indicate the huge presence of HA. The spacing value 3.43 with corresponding crystallographic plane (002), which is the good agreement with hydroxyapatite JCPDS (09-0432) data. Which provide the concept that 0.5 Gy electron beam irradiation gives some modification and formed more HA and collagen in the sample.

It was observed that after 100 cGy, 200 cGy and 500 cGy sample irradiated by MeV electron beam, the XRD Curves show the similar type of change at diffraction angle at $26^\circ \pm 1^\circ$. These diffraction peaks show the presence of collagen- hydroxyapatite composite material [26].

From above XRD study it is very much clear that after 0.5 Gy irradiation, there are more collection both HA and Col bone matrix forming materials in the sample in compare with other doses and virgin sample.

Fourier Transform Infrared Spectroscopy Analysis:

The FTIR spectral measurement of all rabbit bone marrow samples were carried out at the sophisticated analytical instrumentation facility at Institute of Physics Bhubaneswar, by using AVTAR-CSI (Thermo Nicolet) Spectrometer in 4 cm^{-1} (Resolution) and auto gain mode. The spectra were recorded in the mid infrared region $500\text{-}4000 \text{ cm}^{-1}$ in transmittance mode.

The FTIR Spectrum of normal rabbit bone marrow is given in figure 9. The peaks of the virgin sample were characterized by the presence of important functional groups viz. the weaker protein bonds CH₃ bending vibrations at $1457\text{-}1495 \text{ cm}^{-1}$, The C=O (Amide-I) stretching of the peptide linkage and C-N, CNN (Amide- II) at $1578\text{-}1665 \text{ cm}^{-1}$ [27], can be assigned to the protein matrix formed. Amide-I arises from the C=O hydrogen bonded stretching vibrations and Amide-II from the C-N stretching and a CNH bending vibrations. The intense peak at 1347 cm^{-1} reveals the presence of Col and HA composite [26] in the sample. In this FTIR pattern the demonstrated range of 1475 cm^{-1} corresponds to the carbonyl group which contributes to surface polarity [28].

The sample after 0.5 Gy irradiation by MeV electron beam in the FTIR pattern is given in figure 11. The intense peak at frequency band 560 cm^{-1} (peak shown by arrow) signifies the presence of phosphate group in carbonated apatite, clearly suggesting the presence of mineralized extracellular matrix [29] which may help the quicker healing of the fractured bone. This band at 560 cm^{-1} is not visible in control/virgin sample spectrum which indicates that after irradiation by 0.5 Gy dose electron radiation, there is presence of phosphate group which modified the material. The peak at frequency 1031 cm^{-1} signifies the presence of the collagenous matrix but this peak is not seen in control spectrum. The mineral phosphate spectral region ($900\text{-}1200 \text{ cm}^{-1}$) peaks are visible here. Another important peak at 1661 cm^{-1} clearly corresponds to nonreducible collagen cross links in bone [30] which is not visible in control spectrum. The spectral peak at 3530 cm^{-1} signifies the presence of hydroxyl group [31]. Hence it is very much clear that after irradiation with specific dose (0.5 Gy) to the sample there is an appearance of bone forming material like collagen matrix. The peaks at 1276 and 1031 cm^{-1} are attributed to PO_2^- ionized asymmetric and symmetric stretching, respectively [32]. The bands at 3273 and 2841 cm^{-1} are CH₂, CH₃ stretching vibrations of cholesterol and phospholipids respectively.

X-Rays Radiograph Analysis:

The tibia bones of six rabbits were completely broken. Then the bone marrow deposited at the tip of broken bone. After that, three

rabbits were taken for irradiation. The dose 0.5 Gy was delivered to fracture site in one fraction to all three rabbits by using 4 MeV electron beam. So there was a direct interaction between electron beam with bone marrow. The seven days regular X-rays radiological images were taken by C-Arm of all six rabbits. The initial phase of new bone formation is called callus, which is visible at fracture site after 7 days (one rabbit image is given in figure 15) due to electron beam irradiation to all three rabbits. But in the other three control rabbits ,callus is poorly visible (one rabbit image is given in figure 16) at fracture site after 7 days. The irradiated and nonirradiated fractured bones are given in figure 15 and 16 respectively. Clinically it has been seen by palpation that the fracture site is little hard due to callus formation in irradiated site than nonirradiated site. This study has been done only for 7 days and a complete study can be done till complete bone repair. So it is a new and clear concept that the MeV electron beam irradiation with 0.5 Gy dose will enhance the healing process of bone than normal healing process.

Figures and Tables:

Figure 1 : Engineering diagram of Low temperature liquid irradiation cell

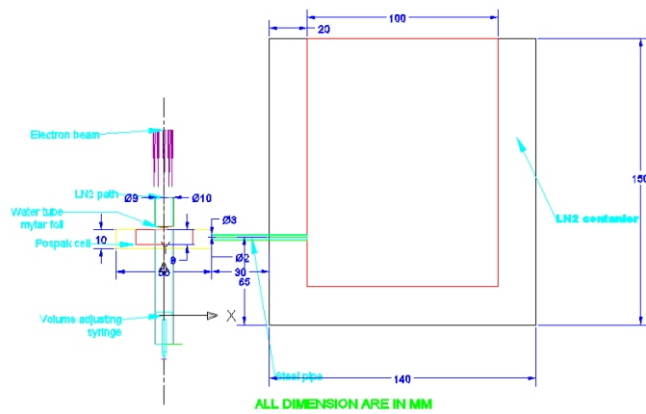


Figure 2 : Diagram of Low temperature liquid irradiation cell

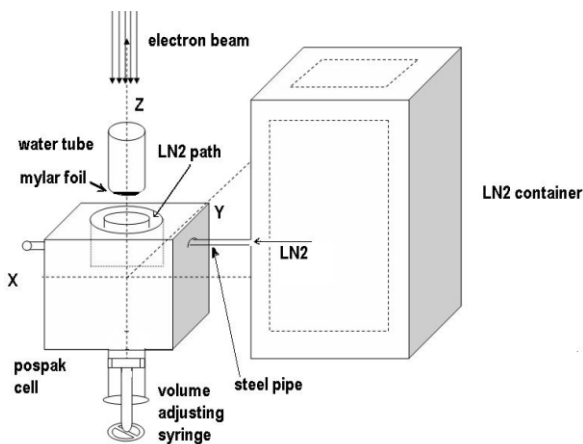


Figure 3 : XRD Curve of 0.1 Gy irradiated Bone marrow

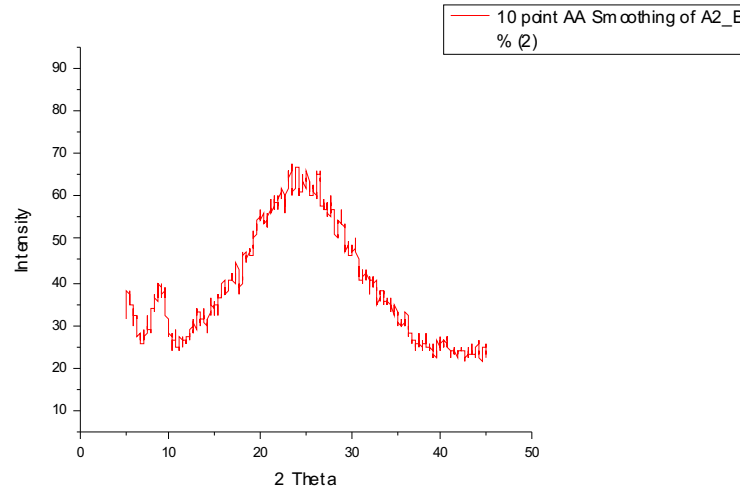


Figure 4 : XRD Curve of Control Bone marrow

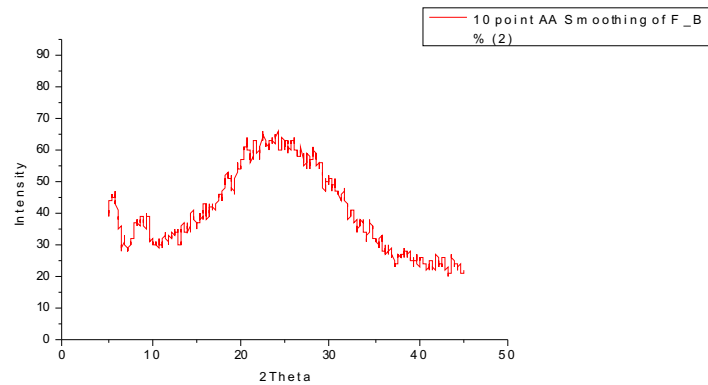
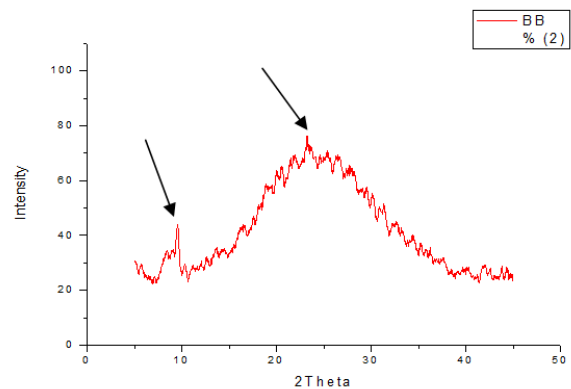


Figure 5: XRD Curve of 0.5 Gy irradiated Bone marrow



4574

Figure 6 : XRD Curve of 1.0 Gy irradiated Bone marrow

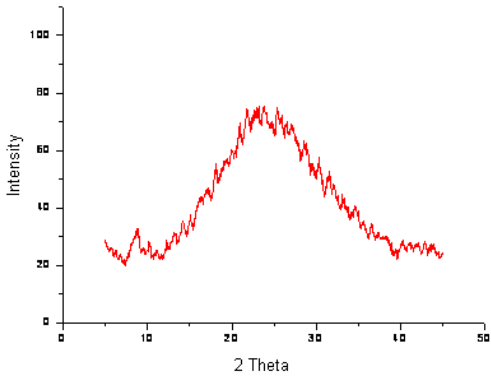


Figure 9 : FTIR Curve of Control Bone marrow

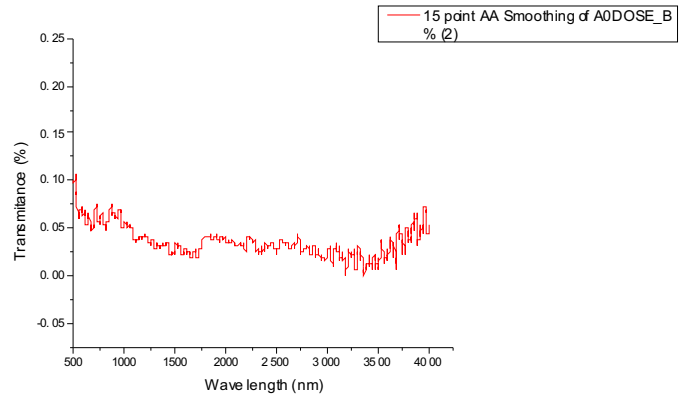


Figure 7 : XRD Curve of 2.0 Gy irradiated Bone marrow

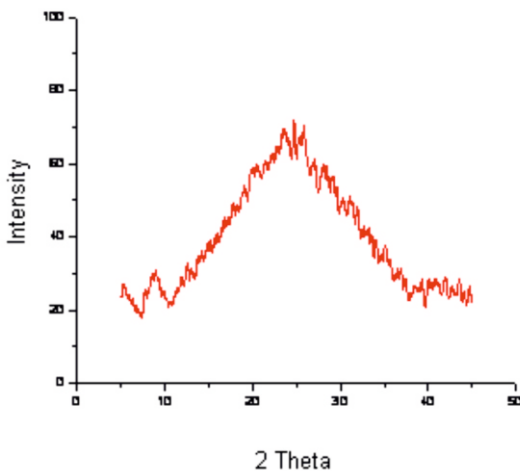


Figure 10 : FTIR Curve of 0.1Gy irradiated Bone marrow

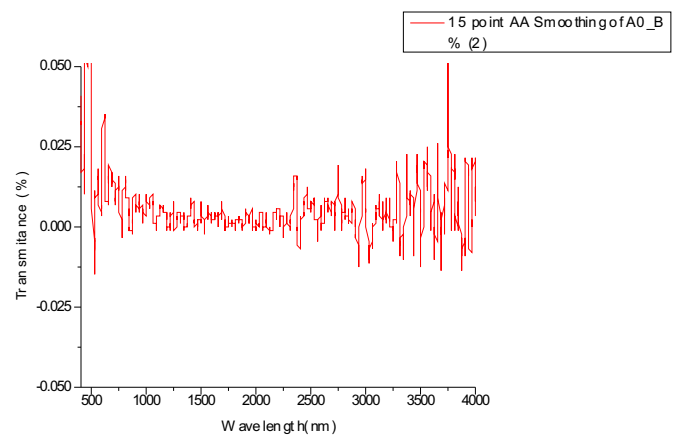


Figure 8 : XRD Curve of 5.0 Gy irradiated Bone marrow

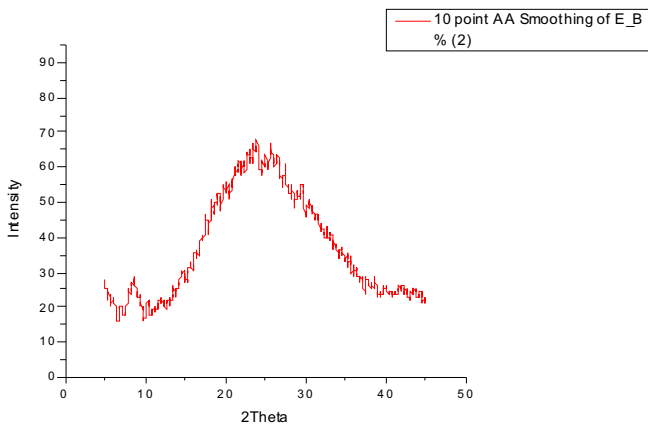


Figure 11 : FTIR Curve of 0.5 Gy irradiated Bone marrow

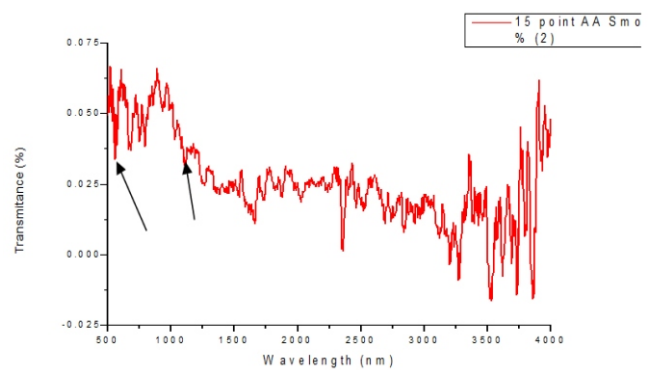


Figure 12 : FTIR Curve of 1.0 Gy irradiated Bone marrow

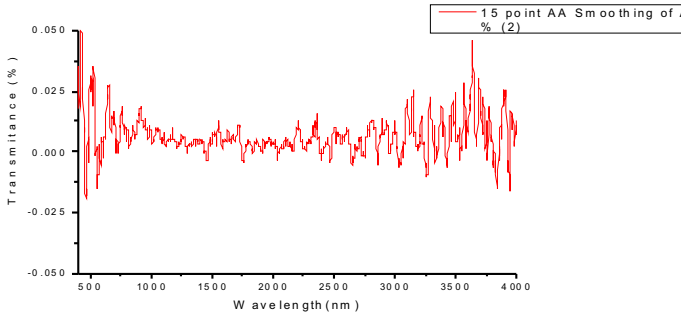


Figure 15 : Callus formation image after 7 days of 0.5 Gy 4 MeV electron beam irradiation

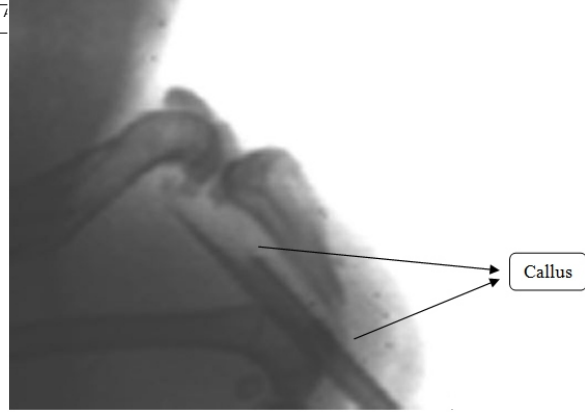


Figure 13 : FTIR Curve of 2.0 Gy irradiated Bone marrow

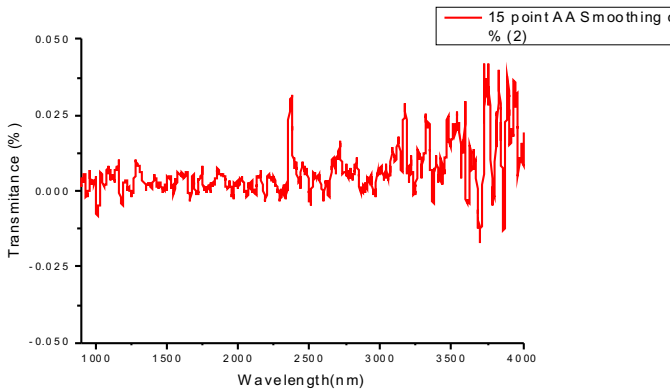


Figure 16 : Callus formation image after 7 days of destruction of bone without irradiation

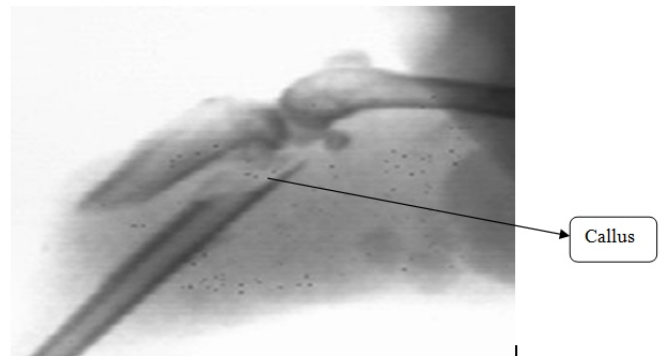


Figure 14 : FTIR Curve of 5.0 Gy irradiated Bone marrow

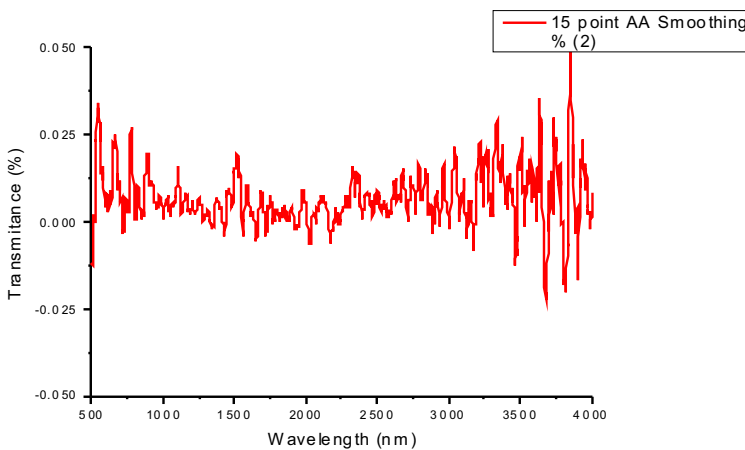


Table No. 1: XRD Curve table of Control Bone marrow

Peak Number	2θ	I	d (Å)
1	5.62	46.29	15.71
2	6.99	32.57	12.63
3	8.91	39.40	9.91
4	14.63	41.71	6.04
5	18.38	53.80	4.82
6	24.08	66.21	3.69

Table No. 2: XRD Curve table of 0.1 Gy Irradiated Bone marrow

Peak Number	2θ	I	d(Å)
1	5.41	37.90	16.32
2	8.817	39.52	10.02
3	20.03	56.72	4-429
4	23.22	66.15	3.82
5	26.52	65.69	3.35
6	28.88	56.06	3.038

Table No. 3: XRD Curve table of 0.5 Gy Irradiated Bone marrow

Peak Number	2θ	I	d(Å)
1	5.62	29.28	15.71
2	8.50	34.62	10.39
3	9.42	43.32	9.38
4	16.53	43.32	5.35
5	23.12	75.87	3.52
6	25.28	70.25	3.52

Table No. 4 : XRD Curve table of 1.0 Gy Irradiated Bone marrow

Peak Number	2θ	I	d(Å)
1	8.81	32.36	10.02
2	10.15	27-87	8.70
3	20.86	68.27	4.25
4	21.88	73.89	4.05
5	25.39	74.46	3.505
6	30.42	57.91	2.93

Table No. 5 : XRD Curve table of 2.0 Gy Irradiated Bone marrow

Peak Number	2θ	I	d(Å)
1	8.81	32.36	10.02
2	10.15	27-87	8.70
3	20.86	68.27	4.25
4	21.88	73.89	4.05
5	25.39	74.46	3.505
6	30.42	57.91	2.93

Table No. 6: XRD Curve table of 5.0 Gy Irradiated Bone marrow

Peak Number	2θ	I	d(Å)
1	6.10	22.39	14.47
2	8.70	28.19	10.15
3	17.56	46.84	5.04
4	23.74	66.72	3.74
5	25.70	66.47	3.46
6	29.50	54.84	3.02

CONCLUSIONS:

The radiation- induced modifications of bone marrow were investigated using X-Ray diffraction (XRD) and Fourier transforms Infrared Spectroscopy (FTIR) spectral analysis techniques. The physical changes of bone healing of the fractured bone after electron beam irradiation was investigated by X-Ray radiological imaging.

As a result of the investigations following conclusions can be drawn.

- i) This study tabulated a very good spectral analysis data (XRD and FTIR) about MeV electron beam irradiation with rabbit bone marrow.
- ii) From XRD study of rabbit bone marrow, it is concluded that due to particular dose of 50 cGy electron beam irradiation, there are more accumulation both HA and Col bone matrix forming materials in the sample in comparison to other doses and virgin sample.
- iii) In the FTIR pattern of the sample after 50 cGy irradiation by MeV electron beam, the intense peak at frequency band 560 cm⁻¹ signifies the presence of phosphate group in carbonated apatite, clearly suggesting the presence of mineralized extracellular matrix which helps quicker healing of the fractured bone.
- iv) Inside fractured long bone, bone marrow is there. When it is irradiated by electron beam with dose 0.5 Gy, there is an interaction of bone marrow with electron beam. So there are more formation of HA and Col bone forming materials as electron beam is of highly charged particles.
- v) Callus is the initial phase of new bone formation. After only seven days of electron beam irradiation to fracture site a visible callus has formed but is not clearly visible in normal fractured bone without irradiation. The callus visibility study has been examined by X-rays radiological images.

The investigated results in this work, particularly after 0.5 Gy electron beam irradiation, indicate that there are more accumulation of bone forming material like both inorganic hydroxyapatite and organic collagen at fracture site which means the quicker healing of fractured bone than without irradiation. This concept can be used for any bone fractured treatment management.

Acknowledgement

Authors would like to thank Doctors of Radiation Oncology and Technical staff of Medical Physics Department and the crew of the LINAC at Hemalata Hospitals and Research Centre, Bhubaneswar. Special thanks are due to Dr. N. N. Mandal of Regional Medical Research Centre, Bhubaneswar for his suggestions and help during experimental work.

REFERENCES :

1. GOLD R S, MAXIM J, HALEPASKA (JR) D J , WALES M E, JOHNSON D A, WILD JR 2005, *J Biomater sci polym*, 16(1) 79-89
2. HERNANDEZ C J, BEAUPRE G S, CARTER D R 2003 *International Journal of Bone*, 32(4) 357-63
3. REYNDERS P 2003 Intra-osseous injection of concentrated autologous bonemarrow in 62 cases of delayed union, *Folia Traumat Lovaniensia* 108-116
4. PORTER S E, HANLEY E N 2001, The musculoskeletal effect of smoking, *J AM Acad Orthop Surg* 9(1) 9-17
5. SROUJI S, LIVNE E 2005 Bone marrow stem cells and biological scaffold for bone repair in aging and disease, *Mech Ageing De* 126(2) 281-287
6. SIM R, LIANG T S , TAY B K 1993 Autologous marrow injection in the treatment of delayed and non-union in long bones , *Singapor Med J* 4(5) 412-417
7. LIANG Y T, ZHANG B X , LU S B 1999 Experimental study and clinical application on osteogenesis of percutaneous autogenous bone marrow grafting in bone defects, *Zhongguo Xiu Fu Chong Jian Wai Ke Za Zhi* 13(3) 148-151
8. CONNOLLY J F, GUSE R, TIEDEMAN J, DEHNER 1991 Autologous marrow injection as a substitute for operative grafting of tibial nonunions, *Clin Orthop Relat Res* 266 259-270
9. YAAKOBI T, MALTZ L, ORON U 1996 Promotion of bone repair in the cortical bone of the tibia in rats by low energy laser (He-Ne) irradiation, *Calcif Tissue Int* 4 297-300
10. LUGER E J, ROCHKIND S, WOLLMAN Y, KOGAN G, DEKEL S 1998 Effect of lowpower laser irradiation on the mechanical properties of bone fracture healing in rats *Lasers , Surg Med*. 22(2) 97-102.
11. SAHOO S K , RATH A K , MUKHARJEE R N , MALLICK B 2012 Commissioning of a Modern LINAC for Clinical Treatment and Material Research, *International Journal of Trends in Interdisciplinary Studies*. Volume 1 issue 10
12. CARLO M , MARIA D , STEFANIA N ,SETTIMIO M , RDY H W 2003 Rietveld Refinement on X-ray Diffraction patterns of Bioapatite in Human Fetal Bones *Biophysical Journal* 84 2021-2029.
13. FENGLIANG Z , ANNING W , ZHIHUA L , SHENGWEN H , D LJUN S 2011 Preparation and Characterisation of collagen from fresh water fish scales *Food and Nutrition science* 2 818-823.
14. PALANISAMY T, NARAYANAN T, PRADHAN B K, AJAYAN M 2012 Collagen based magnetic nanocomposites for oil removal application *Sci Rep*. 2 : 230.
15. MICHEL I , ISMAELA F , SIMONA S , GIORGIO T , NORBERTO R 2012 Electrospun Nanostructured fibers of collagen- Biomimetic apatite on titanium Alloy, *Bioinorganic chemistry and Applications* 10 1155/123953.
16. SANKARI G , AISHWARYA T S , GUNASEKHARAN S, SURAPANENI K M 2011 Analysis of multiple myeloma by FTIR Spectroscopy coupled with statistical Analysis, *Journal of Clinical and Diagnostic research* 55 1001-1007
17. UVANESWARY S , RAO H , RAGHAVENDRAN B , IBRAHIM N S , MURALI R M , MERICAN A, MKAMARUL T 2013 A Comparative Study on Morphochemical Properties and Osteogenic Cell Differentiation within bone graft and coral graft culture systems, *Int. J. Med. Sci.* 10(12) 1608-1614.
18. BOSKEY A L 1998 Biominerization: conflicts, challenges, and opportunities *J Cell Biochem Suppl*, 30-31 83-91.
19. PASCHALIS E P, VERRDELIS K, DOTY S B, BOSKEY A L, MENDELSON R , YAMAUCHI M 2001 Spectroscopic Characterization of Collagen Cross-Links in Bone, *Journal of Bone and Mineral Research* 16 1821-1828.
20. CHETTRI B , NANDI S K , CHAND A , BEGAM H 2012 Bone ingrowth to insulin like Growth factor-1 loaded zinc doped Hydroxyapatite Implants: an invivo Study *Scientific Reports* vol 1, issue 4.
21. KRUPNIK E , JACKSON M , BIRD R , SMITH I , MANTSCH H 1998 Investigation into the infrared spectroscopic characteristics of normal and malignant colonic epithelium", *SPIE* 3257 307-310.